



# Experimental study on low-speed lubrication characteristics of large tilting pad bearings

Yang Peiji<sup>1</sup> · Sun Quan<sup>1</sup> · Chen Runlin<sup>2</sup> · Zhao Zhiming<sup>1</sup> · Yao Bing<sup>3</sup> · Pang Kai<sup>1</sup> · Sun Jiangong<sup>1</sup>

Received: 2 April 2024 / Accepted: 23 July 2024 / Published online: 10 August 2024

© The Author(s), under exclusive licence to The Brazilian Society of Mechanical Sciences and Engineering 2024

## Abstract

Large generator sets may experience boundary lubrication between the bearing and the shaft during startup, shutdown, or low-speed cranking. This can lead to localized wear or damage to the bearing and rotor surfaces, potentially causing safety accidents in the unit. In this paper, the lubrication properties of the unevenly distributed six-watt tilting pad bearings in an in-service unit are analyzed through theoretical calculations. The analysis focuses on parameters such as film thickness and temperature rise under low-speed operating conditions. Subsequently, a full-size test rig is set up to examine the lubrication properties of bearings made of two materials—Babbitt alloy and polytetrafluoroethylene (PTFE). The tilting pad temperatures, film thicknesses, and vibration characteristics of the bearings are tested under actual operating conditions. The test results show that: The designed bearing does not exhibit wear under low-speed conditions (40 r/min); the bearing made of PTFE material has lower temperatures compared to those made of Babbitt alloy, with higher pivot film thickness than that of the Babbitt alloy; the bearing pivot film thickness value using VG68 oil is larger than that of VG46; and the values of the temperature of the tilting pad measurement point are larger than that of VG46. This research paper validates the feasibility of the bearing design scheme for this unit and provides data support for the design and safe operation of similar units.

**Keywords** Tilting pad bearings · Low-speed cranking · Babbitt alloys · PTFE material

## 1 Introduction

With the advent of the Fourth Industrial Revolution, green and intelligent have become one of the mainstream directions for the development of mechanical products. Green energy in the field of power machinery, such as nuclear energy, hydroelectric power, wind power, and other green energy, has become a major trend in the development of the unit with the increase in capacity and power generation efficiency and the subsequent increase in the size of the rotor and bearings, which puts forward stringent requirements on the bearing performance as well as the stability

and reliability of the rotor bearing system. [1, 2] Tilting pad journal bearings are widely used in rotating machinery rotor systems for high parameter operating conditions due to their inherent dynamic stability characteristics. In order to select and design a tilting pad bearing that is compatible with a given operating condition, it is necessary to obtain accurate properties such as bearing temperature, oil film thickness, stiffness, damping coefficient, etc. [3–5].

With the advancement of computer and testing technologies, issues related to tilting pad bearings in practical applications have been identified and addressed, and new models for solutions have been established. The mathematical model for the fluid lubrication of tilting pad bearings has evolved from a simple two-dimensional thermo-hydrodynamic analysis model to a complex three-dimensional thermo-hydrodynamic analysis model, and further to a complex three-dimensional and simplified thermo-elasto-hydrodynamic analysis model [6, 7]. This has continuously improved both calculation accuracy and speed. The structural parameters of the bearing, such as the pad wrap angle, length-to-diameter ratio, bearing clearance, pivot location, and pivot flexibility, have a significant impact on bearing performance and can be optimized to

Technical Editor: Daniel Onofre de Almeida Cruz.

✉ Yang Peiji  
ypjhny@163.com

<sup>1</sup> College of Mechanical & Electrical Engineering, Shaanxi University of Science and Technology, Xi'an, China

<sup>2</sup> School of Mechanical and Precision Instrument Engineering, Xi'an University of Technology, Xi'an, China

<sup>3</sup> Zhejiang Zhuji Bearing Bush Factory Co., Ltd., Zhuji, China

improve bearing performance [8, 9]. Additionally, rotor tilt and misalignment also significantly affect the bearings [10, 11]. Under high-speed conditions, tilting pad bearings operate in a turbulent state, leading to increased frictional power loss, lubrication oil flow, and bearing temperature, which deteriorates bearing lubrication performance [12, 13]. Over the years, extensive theoretical and experimental research has provided important evaluation criteria for the design and reliable application of tilting pad bearings, forming a common knowledge base. As units develop toward higher speeds and higher power densities, the performance optimization of tilting pad bearings has reached the material limits, making the improvement of bearing pad materials one of the main research directions in recent years [14, 15]. Xu JM et al. [16] covered the surface of modified superconducting tilting pads with a thin layer of impregnated graphite and replaced the nickel coating of the magnet with a chromium coating, resulting in improved safety for liquid rocket engines through this anti-friction design method. Podrabinnik et al. [17] experimentally studied the tribological behavior of an Al–Sn–Pb–Si–Cu–Mg–Zn aluminum alloy against steel and conducted tests on journal-bearing friction pairs. Madej et al. [18] investigated the influence of the chemical composition of two tin-based bearing alloys (B89 and B83) on their tribological performance, finding that the precipitation of the SnSb phase in the B83 alloy is the main factor affecting the wear resistance of bearing alloys. Mosleh et al. [19] developed an alloy with excellent tribological performance and high mechanical properties for engine bearings and accurately predicted the characteristics of the new alloy with low error levels through experiments. On the other hand, CFD simulation is an important method for studying complex working conditions and structures. Wang et al. [20] proposed a method to study the hydrodynamic performance of sliding bearings by using CFD simulation of microflow in texture, which provides a basic reference and theoretical basis for the design and optimization of journal bearings; Guglielmo et al. [21] designed a highly efficient flexible multi-body model of bearings that can be computed by CFD and can be used in different engineering fields. The application of new materials has improved bearing performance, especially raising the limits of stable operation at high temperatures.

Despite the continuous development of theoretical research considering multiple factors, the existing theories still struggle to support specialized working conditions and bearing structures as the application conditions become more extreme and the dimensions, structures, and materials of bearings change accordingly. It is necessary to accurately determine the performance of bearings through full-scale, all-condition testing [22, 23].

Based on theoretical research considering the heat conduction and thermal deformation of the pad, this paper focuses on a large in-service generator's unequally distributed six-pad

tilting pad bearing. A full-scale test rig is established to primarily study the lubrication performance of bearings made from two materials, Babbitt alloy and PTFE, under low-speed conditions. The study includes evaluating parameters such as film thickness, pad temperature, and vibration, to assess the safety of the bearings during startup, shutdown, or low-speed turning.

## 2 Modeling and analysis of tilting pad bearings with different materials

### 2.1 Modeling and calculation process of tilting pad bearings with different pad surface materials

#### 2.1.1 Generalized Reynolds equation

Assuming a lubricant incompressible fluid and not considering inertial and volumetric forces, the steady state Reynolds equation containing the turbulence correction factor is: [24]

$$\frac{\partial}{\partial x} \left( F_2 \frac{\partial p}{\partial x} \right) + \frac{\partial}{\partial z} \left( F_3 \frac{\partial p}{\partial z} \right) = U \frac{\partial}{\partial x} \left( h - \frac{F_1}{F_0} \right) + \left[ 1 + \frac{1}{R} \left( h - \frac{F_1}{F_0} \right) \right] V \quad (1)$$

In the formula,

$$F_0 = \int_0^h \frac{dy}{\mu}; F_1 = \int_0^h \frac{y dy}{\mu}; F_2 = \frac{1}{K_x} \int_0^h \frac{y}{\mu} \left( y - \frac{F_1}{F_0} \right) dy;$$

$$F_3 = \frac{1}{K_z} \int_0^h \frac{y}{\mu} \left( y - \frac{F_1}{F_0} \right) dy \quad ;$$

$p$ —oil film pressure/Pa;  $h$ —oil film thickness/ $\mu\text{m}$ ;  $\mu$ —lubricant dynamic viscosity/Pa·s;  $U$ —tangential velocity of journal surface;  $V$ —radial velocity of journal surface;  $R$ —radius of inner arc of tilting pad;  $K_x$ —tangential turbulence coefficient (right-angle coordinate system); and  $K_z$ —axial turbulence coefficient (right-angle coordinate system).

#### 2.1.2 Energy equation

When the journal at the bearing is in a stable state, the heat generated by bearing friction and convection and conduction to achieve thermal equilibrium, the formation of a stable temperature field, the temperature field is determined by the energy equation. Do not consider the influence of heat radiation, and the working condition is constant motion; do not take into account the change of temperature along the axial direction; the energy equation under the right-angle coordinate system is:

$$\rho c_v \left[ u \frac{\partial T}{\partial x} + v \frac{\partial T}{\partial y} \right] = \kappa_0 \frac{\partial^2 T}{\partial y^2} + \mu \left[ \left( \frac{\partial u}{\partial y} \right)^2 + \left( \frac{\partial w}{\partial y} \right)^2 \right] \quad (2)$$

In the formula,

$\rho$ —lubricant density;  $c_v$ —specific heat capacity of the lubricant;  $u$ ,  $w$ , and  $v$ —flow rate of the lubricant along the  $x$ ,  $z$ , and  $y$  directions, respectively;  $T$ —temperature of the lubricant; and  $\kappa_0$ —thermal conductivity of the lubricant.

### 2.1.3 Tilting pad heat conduction equation

When the shaft journal at the bearing is in a steady state, the heat generated by bearing friction and dissipated through convection and thermal conduction reach equilibrium, forming a stable temperature field. This temperature field can be determined by the energy equation:

$$\frac{\partial^2 T}{\partial r^2} + \frac{1}{r} \frac{\partial T}{\partial r} + \frac{1}{r^2} \frac{\partial^2 T}{\partial \varphi^2} = 0 \tag{3}$$

In the formula,

$$\kappa_p \frac{\partial T}{\partial r} \Big|_{r=R+H_b} = \lambda(T_a - T), \quad \kappa_p \frac{\partial T}{\partial \varphi} \Big|_{\varphi=\varphi_2} = \lambda(T_a - T)$$

$T_a$ —ambient temperature,  $H_p$ —tilting pad temperature,  $\kappa_p$ —tilting pad heat transfer coefficient, and  $\lambda$ —tilting pad backing heat dissipation coefficient.

The pad surface material of the PTFE tilting pad bearing is composed of PTFE material filled into a copper wire mesh. When calculating thermal resistance, these two layers are equivalent to a material with the same thermal conductivity coefficient:

$$\text{Thermal resistance} = \frac{h_a + h_b}{k_e} = \frac{h_a}{k_a} + \frac{h_b}{k_b} \tag{4}$$

In the formula,

$k_a$ ,  $k_b$ —the thermal conductivity of the two materials,  $h_a$ ,  $h_b$ —the thickness of the two materials, and  $k_e$ —the equivalent thermal conductivity of the composite layer formed by the two materials.

PTFE tilting pad bearing heat conduction can be considered as a PTFE layer plus the steel base of the two layers of material heat conduction and the two layers of material in the middle of the heat transfer continuity. The heat conduction equation of the PTFE tilting pad bearing is as follows:

$$\begin{aligned} \frac{\partial^2 T_e}{\partial r_e^2} + \frac{1}{r_e} \frac{\partial T_e}{\partial r_e} + \frac{1}{r_e^2} \frac{\partial^2 T_e}{\partial \varphi^2} &= 0 \\ \frac{\partial^2 T_m}{\partial r_m^2} + \frac{1}{r_m} \frac{\partial T_m}{\partial r_m} + \frac{1}{r_m^2} \frac{\partial^2 T_m}{\partial \varphi^2} &= 0 \\ ke \frac{\partial T_e}{\partial r_e} \Big|_{r_e=R_o} &= km \frac{\partial T_m}{\partial r_m} \Big|_{r_m=R_o} \end{aligned} \tag{5}$$

### 2.1.4 Thermo-elastic deformation equation of tilting pad

The thermo-elastic deformation of the tilting pad is the sum of elastic and thermal deformation, and the thermo-elastic deformation equation is as follows:

$$\frac{1}{R^2} \frac{d\Delta}{d\varphi^2} = \frac{M}{EI} + 1.5 \frac{q}{GA} + \frac{\alpha \Delta T}{H_b} \tag{6}$$

In the formula,

$\Delta$ —thermo-elastic deformation;  $A$ —tilting pad cross-sectional area,  $A = LH_b$ ; and  $I$ —moment of inertia of tilting pad section,  $I = \frac{LH_b^3}{12}$ . The bending moment from the inlet end of the tilting pad to the pivot point is  $M(\varphi) = \frac{R^2 L \omega \mu_0}{\psi^2} \int_0^{\varphi-\varphi_1} q(\xi) \xi d\xi$ ;  $q$ —force distribution on the axial neutral plane of the tilting pad,  $q = \frac{L \omega \mu_0}{\psi^2} \int_0^1 \bar{p} d\lambda$ ; and  $\Delta T$ —temperature difference between tilting pad face and back.

### 2.1.5 Film thickness equation

When the tilting pad exhibits thermo-elastic deformation, the relationship between the journal and the tilting pad's geometry allows the derivation of the bearing film thickness equation. After correction, the film thickness equation for the tilting pad bearing under the thermo-elastic hydrodynamic model is expressed as follows:

$$h_i = c_p - (c_p - c_b) \cos(\beta_i - \varphi) + e \cos(\varphi - \theta) + r \delta_i \sin(\beta_i - \varphi) + \Delta \tag{7}$$

In the formula,

$C_p$ —shaft radius clearance and  $\delta_i$ —tilting pad pendulum angle.

### 2.1.6 Temperature–viscosity equation

The viscosity of lubricating oil is significantly affected by temperature and is sensitive to changes in temperature. In this paper, the following temperature–viscosity equation is used for performance calculations considering the temperature–viscosity relationship:

$$\mu = ae^{-bT} + \frac{c}{T} \tag{8}$$

In the formula,

$\mu$ —viscosity of lubricating medium when the temperature is  $T$ ;  $a$ ,  $b$ , and  $c$  are coefficients to be determined, and the values of  $a$ ,  $b$ , and  $c$  are different for different oils.

### 2.1.7 Calculation process

Simultaneous Eqs. (1–1) to (1–8) can be used to establish a thermo-viscoelastic hydrodynamic lubrication analysis model for the tilting pad bearing. This model considers the heat conduction of the pad surface and pad block, as well as the deformation under heavy loads, making the calculation results more consistent with actual conditions.

The calculation process of the fluid dynamic lubrication model for tilting pad sliding bearings is a multiple iteration process of the basic equations. The flowchart of the program calculation is shown in Fig. 1.

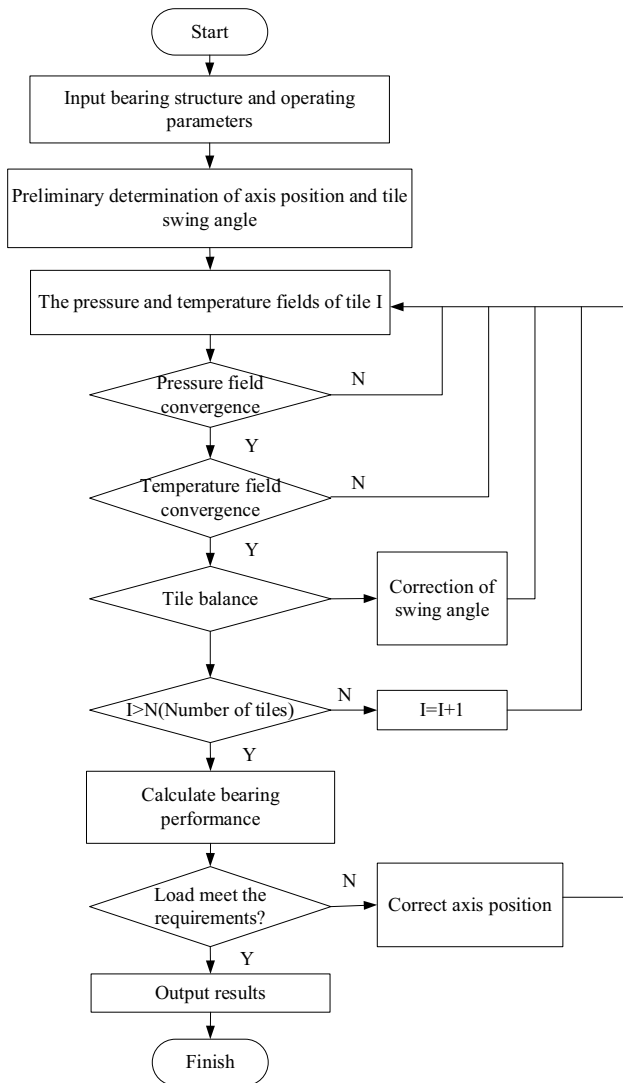


**Fig. 1** The calculation process of the fluid dynamic lubrication model for tilting pad sliding bearings

### 2.2 Effect of bearings on rotor vibration

An isotropic rotor excited by inertial forces associated with mass imbalance is modeled as follows [25]:

$$M\ddot{x} + D_s\dot{x} + Kx = mr\omega^2 e^{j(\omega t + \delta)} \tag{9}$$

The rotor response is defined as:

$$x = Ae^{j(\omega t + \varphi_0)}$$

In the formula,

A and  $\varphi_0$  are the amplitude and phase of the rotor response, and the magnitude of the response will depend on the rotational speed. The maximum amplitude occurs when the operating speed equals the natural frequency of the rotor at  $\sqrt{K/M}$ :

$$A = \frac{F}{\sqrt{(K - M\omega^2)^2 + D_s^2\omega^2}} \tag{10}$$

$$\varphi_0 = \arctan \frac{-D_s\omega}{K - M\omega^2}$$

According to Eqs. (1–10), the amplitude (A) is related to the external force (F), bearing stiffness (K), damping (Ds), rotor mass (M), and operating speed. For large, low-speed, steady-operating rotor systems, where the external force (F) and rotor mass (M) are constant and the operating speed is below the critical speed, the rotor behaves rigidly. In this scenario, the rotor and bearings are weakly coupled, and the rotor system's vibration is sensitive to external structural parameters, such as bearing clearance and installation. However, it is less affected by changes in speed and load.

### 2.3 Lubrication performance analysis of large tilting pad bearings under low-speed operating conditions

For large generator sets in service using tilting pad bearings, a non-uniform arrangement is adopted: four pads at the bottom and two pads at the top. Low-pressure oil inlets are designed between adjacent pads, and high-pressure oil inlets are designed in the middle of each of the two bottom pads. The structure is shown in Fig. 2. There are two kinds of tilting pad surface materials: Babbitt alloy (ZSnSb11-6) and PTFE, and the specific structural parameters are shown in Table 1.

According to the structural parameters of the bearings, the lubrication performance of the bearings under low-speed working conditions is calculated using the method in Sect. 1.1. In order to correspond with the following experimental contents, the pivot film thickness point and the temperature measuring point (the angle from the measurement

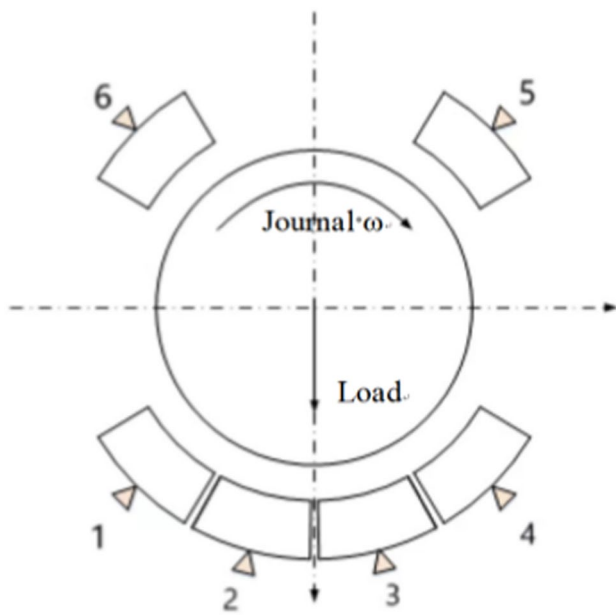


**Fig. 2** Schematic structure of tilting pad bearing

point to the oil inlet edge is at 75% of the wrap angle of tilting pad) of the four tilting pads in the load-bearing area under different loads and different rotational speeds are calculated when PTFE and Babbitt alloy bearings are lubricated by VG46/VG68, respectively. Since pad 1 and pad 4 are symmetrical and pad 2 and pad 3 are symmetrical, ignoring factors such as pivot friction, the theoretical values of the pivot film thickness and the pad measurement point temperature for pad 1 and pad 4, as well as for pad 2 and pad 3, are equal, as shown in Figs. 3 and 4. The film thickness at the pivot point decreases gradually with the increase in load, and under the same load, the larger the rotational speed, the greater the pivot point film thickness. The temperature at the measuring point of the tiling pad increases gradually with the increase in load, and under the same load, the higher the rotational speed, the higher the temperature of the tiling pad; under the same working conditions (rotational speed and load), the pivot film thickness of bearings adopting VG68 is 0.0067 mm thicker than that of VG46, and the

temperature of the measuring point of bearings adopting VG68 is about 1.0067 mm higher than that of VG46. Under the same working conditions (speed and load), the thickness of the film at the pivot point of VG68 bearing is 0.0067 mm thicker than that of VG46, and the measured temperature of VG68 bearing is about 1.07 °C higher than that of VG46, while the thickness of the film at the pivot point of PTFE tiling pad-lined bearing is 0.0304–0.2045 mm thicker than that of the Babbitt alloy tiling pad-lined bearing, and the measured temperature of the pivot point of VG68 bearing is 34.02–38.88 °C (the temperature of the oil inlet is 32 °C), which is 0.3–1.94 °C lower than that of Babbitt alloy tilting pad bearing.

### 3 Test system and test program

#### 3.1 Test rig

According to the actual unit, a full-size tilting pad bearing test rig was designed as shown in Fig. 5 (Fig. 6 shows the photograph of the test rig), which can simulate the operation of this bearing under low-speed working conditions. The test rig mainly consists of four parts: drive system, loading system, lubrication system, and inspection system. The drive motor is a frequency conversion motor with a power of 75 kW and a speed range of 40–100 r/min. The loading system adopts a hydraulic cylinder loading with a maximum load of 190 kN, and the lubricant grades are VG46 and VG68.

During the test, the inlet oil temperature is controlled near 32 °C; in order to ensure adequate lubrication of bearings and journals, the high-pressure jacking oil is turned on when the rotor is rotating, so that the rotor is in a floating state, and the high-pressure jacking oil is canceled when the shaft speed is increased to 40 r/min. Low speeds are set at 40 r/min to 100 r/min, increasing by 20 r/min each time, with each speed maintained for 0.5 h. During the stable operation at each speed, loads of 40 kN, 60 kN, 80 kN, 100 kN, 120 kN, 140 kN, and 150 kN were applied to test the temperature

**Table 1** Basic parameters of tilting pad bearings of two materials

Parameter item/unit	1# bearing	2# bearing
Bearing diameter/mm	500	500
Bearing tilting pad length/mm	200	200
Number of tilting pads	6	6
Wrap angle of tilting pad/°	28	28
Angular coordinates of pivot point/°	15/45/135/225/315/345	15/45/135/225/315/345
Oil	VG46/VG68	VG46/VG68
Shingle material	ZSnSb11-6	PTFE
Load/kN	See below for loads	

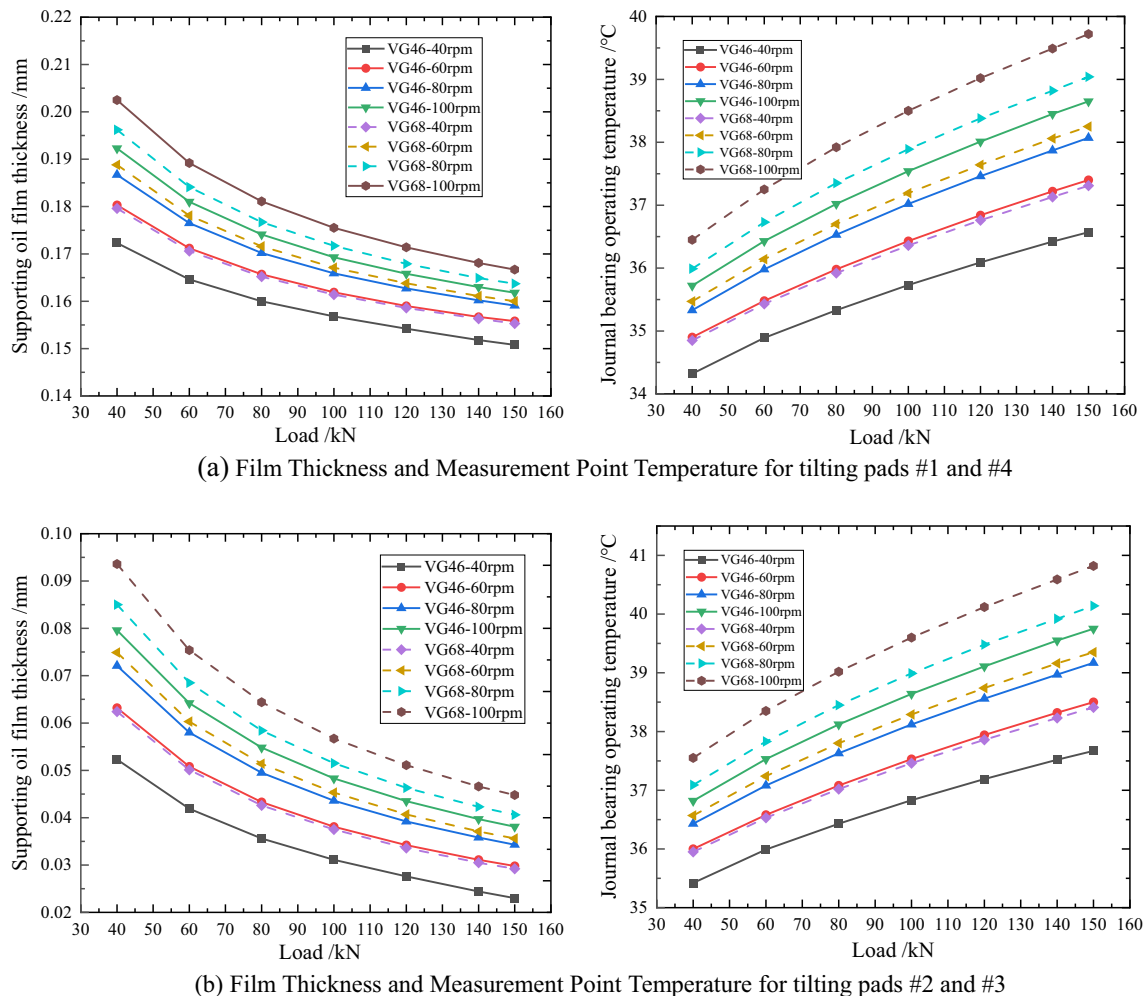


**Fig. 3** Lubrication performance of tilting pad bearings with Babbitt alloy tiling pad liners at low-speed operating conditions

at the measuring point of the tiling pads, the film thickness at the pivot point, and the data of axial vibration, respectively.

### 3.2 Pivot film thickness and vibration test program

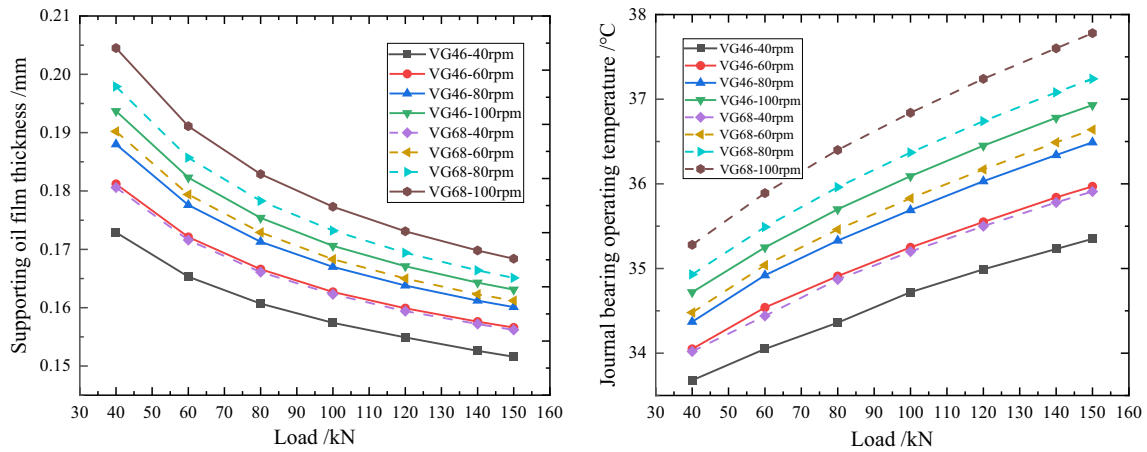
The pivot film thickness is directly measured by eddy current displacement sensor; the sensor model is: BENTLY-3300XL-8 mm, sensitivity is 7.874 V/mm, and linear range is 0–2 mm. The sensor is fixedly mounted on the end face of the base, with a total of four measurement points, two for each bearing, arranged in the bottom of the bearing, and the vertical direction of the symmetrical arrangement of 23°; the direction of the sensor is along the center of the bearing, as shown in Fig. 7. The pivot point film thickness is the sensor test value minus the sensor test calibration value when the rotor is stationary.

The vibration sensors are arranged on the bearing housing, and the sensors are distributed on the top and both sides of the bearing housing along the axial direction, with a total

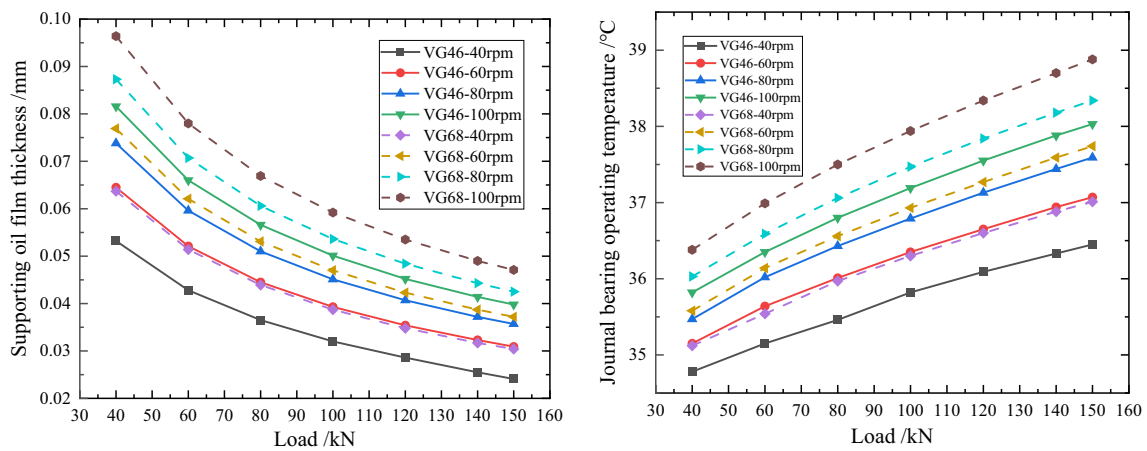
of four sensors, of which I# and II# are the horizontal vibration sensors, and III# and IV# are the vertical vibration sensors, as shown in Fig. 8 in detail.

### 3.3 Tiling pad temperature test program

The bearing pad temperature is measured directly using a temperature sensor. The sensor type is a PT100 5mm platinum resistance temperature sensor, with a temperature range of -100–400 °C and an accuracy of 0.1 °C. Temperature measurement holes are set on the lower pad of the tilting pad bearing, with the four temperature measurement points positioned at an angle of 21° from the oil inlet edge (covering 75% of the pad arc). Based on the size of the sensor, the diameter of the temperature measurement hole is determined to be a 6mm blind hole, with the bottom of the hole approximately 7.5 mm from the bearing pad surface. The arrangement and installation of the temperature measurement points for the two bearings are shown in Fig. 9.



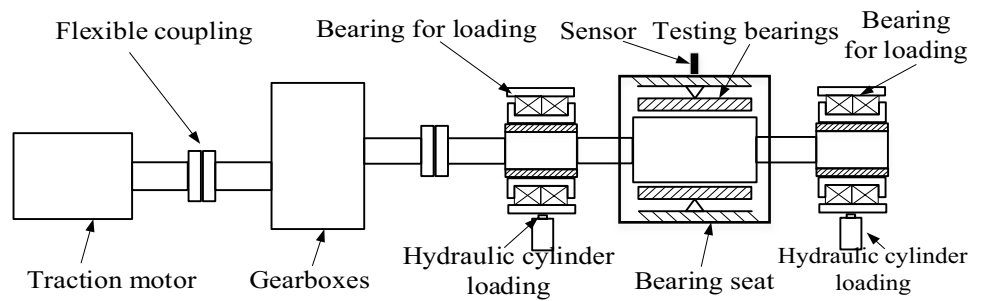
(a) Film Thickness and Measurement Point Temperature for tilting pads #1 and #4



(b) Film Thickness and Measurement Point Temperature for tilting pads #2 and #3

Fig. 4 Lubrication performance of tilting pads bearing with PTFE tiling pad lining at low-speed condition

Fig. 5 Bearing test rig system structure schematic diagram



### 4 Test results and analysis

To study the lubrication characteristics and vibration characteristics of different oils and bearing pad materials at low speeds, the pivot film thickness and the temperature at the measurement points of the four tilting pads in the load zone and the vibration velocity in the horizontal and

vertical directions were tested and analyzed at an operating speed of 40 rpm.

#### 4.1 Pivot point film thickness test results and analysis

The comparative data of the pivot film thickness between the test results and theoretical values for bearings with different

**Fig. 6** Bearing test rig photograph

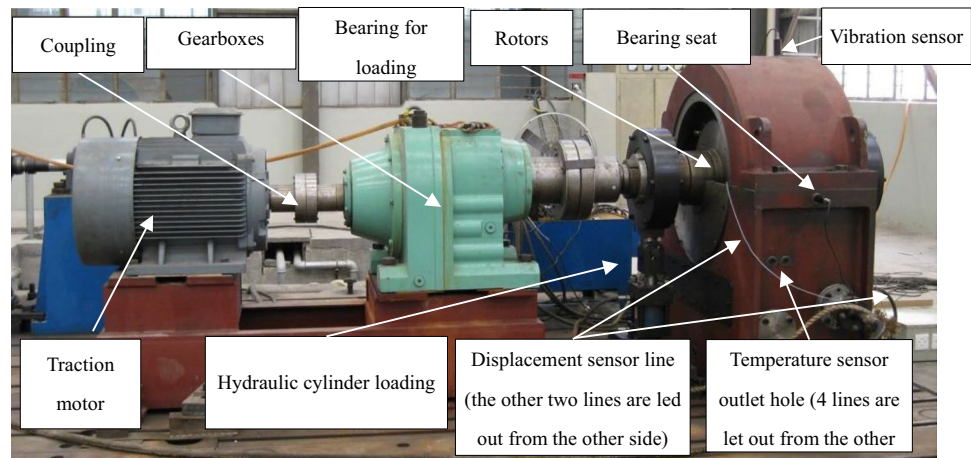
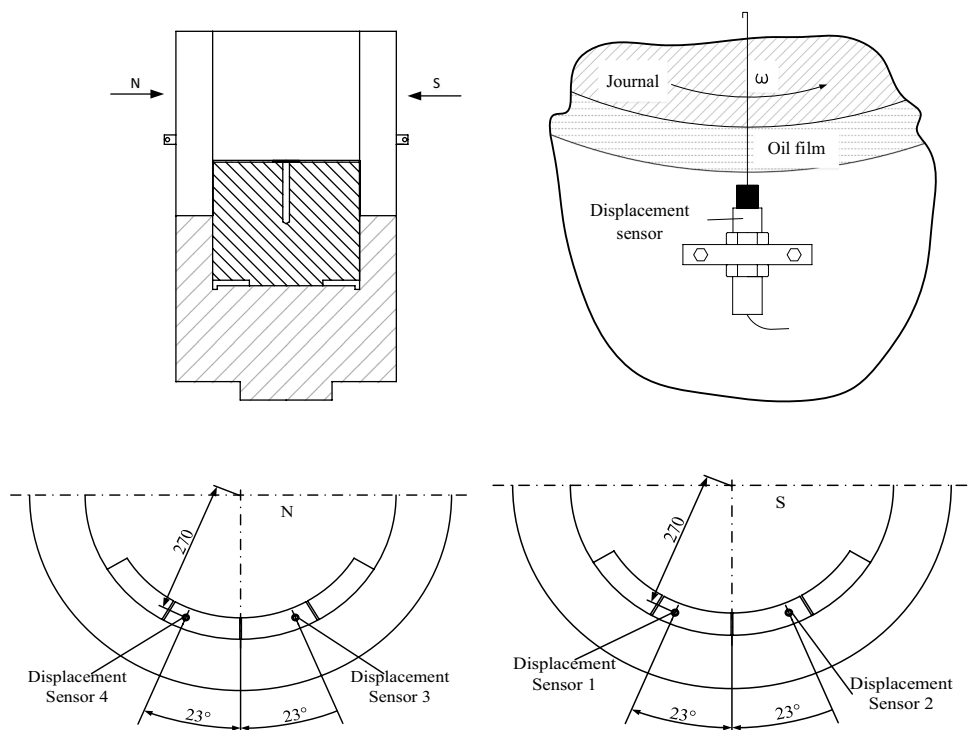


**Fig. 7** Schematic diagram of the bearing displacement test transducer position



pad materials (probes 1 and 4) are shown in Fig. 10. As the load increases, the measured values of the pivot film thickness decrease. The pivot film thickness values for VG68 oil are generally larger than those for VG46 oil, and the thickness for plastic pads is larger than that for alloy pads. For every 10kN increase in load, the film thickness decreases by approximately 0.02 mm. Load range of 40–150 kN: The pivot film thickness of alloy pads lubricated with VG46 oil decreased from 0.2067 to 0.1387 mm and with VG68 oil from 0.2402 to 0.1552 mm. The deviations between the pivot film thickness measured by probe 1 and probe 4 and the theoretical values were 3.6% and 5.5%, respectively, for VG46 oil lubrication and 7.8% and 0.4%, respectively, for

VG68 oil lubrication. The pivot film thickness of plastic pads lubricated with VG46 oil decreased from 0.2315 to 0.1516 mm and with VG68 oil from 0.2064 to 0.1584 mm. The deviations between the pivot film thickness measured by probe 1 and probe 4 and the theoretical values were 7.2% and 0.6%, respectively, for VG46 oil lubrication and 8.0% and 2.2%, respectively, for VG68 oil lubrication. These values are close to theoretical calculations, showing consistent variation patterns.

The comparative data of the pivot film thickness between the test results and theoretical values for bearings with different pad materials (probes 2 and 3) are shown in Fig. 11. As the load increases, the measured values of the pivot film



**Fig. 8** Bearing vibration test sensor location diagram

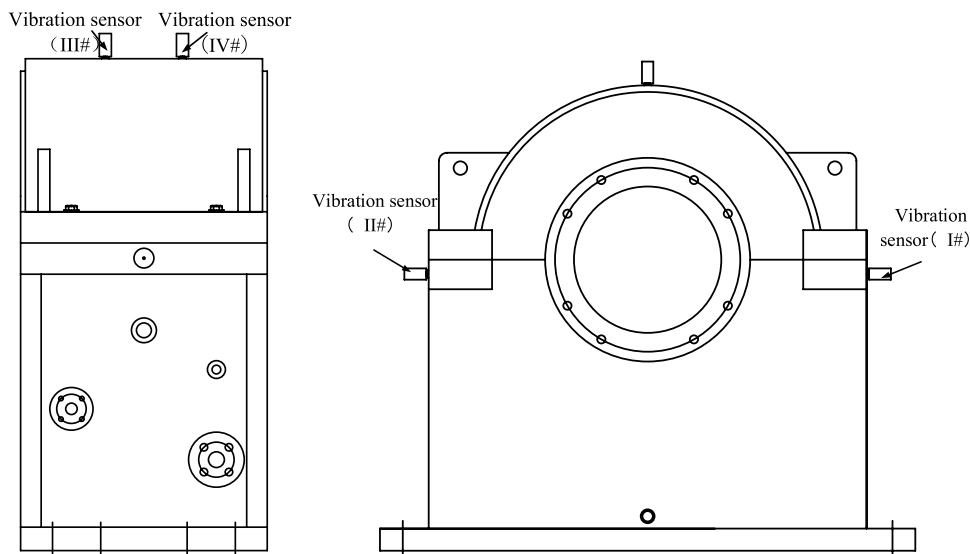
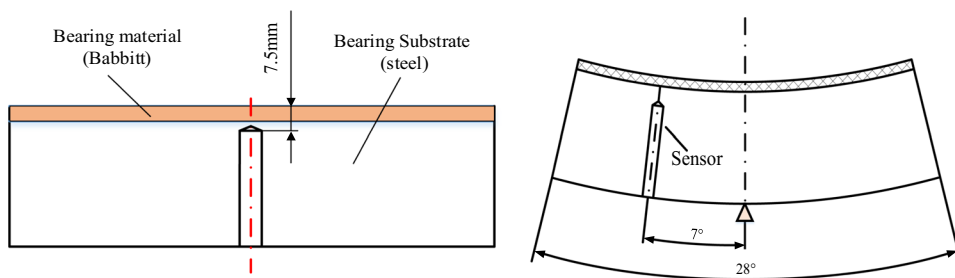
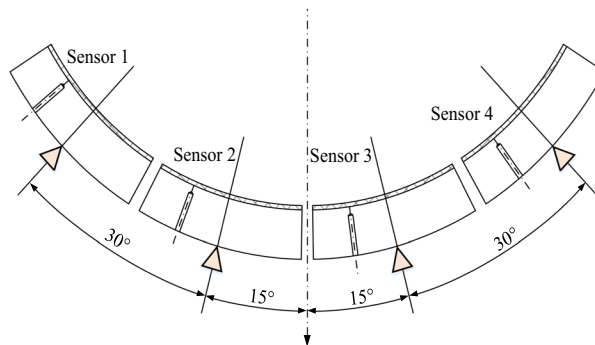


**Fig. 9** Bearing tiling pad temperature test program and temperature measurement hole structure



( a ) Schematic structure and parameters of the temperature measuring



( b ) Temperature measurement hole arrangement scheme

thickness decrease. The pivot film thickness values for VG68 oil are generally larger than those for VG46 oil, and the thickness for plastic pads is larger than that for alloy pads. For every 10kN increase in load, the film thickness decreases by approximately 0.01 mm. Load range of 40–150 kN: The pivot film thickness of alloy pads lubricated with VG46 oil decreased from 0.0443 to 0.0283 mm and with VG68 oil from 0.0502 to 0.0292 mm. The deviations between the pivot film thickness measured by probe 1 and probe 4 and

the theoretical values were 0.3% and 9.8%, respectively, for VG46 oil lubrication and 15.2% and 13.3%, respectively, for VG68 oil lubrication. The pivot film thickness of plastic pads lubricated with VG46 oil decreased from 0.0519 to 0.0319 mm and with VG68 oil from 0.0475 to 0.0216 mm. The deviations between the pivot film thickness measured by probe 1 and probe 4 and the theoretical values were 7.2% and 0.6%, respectively, for VG46 oil lubrication and 8.2% and 2.3%, respectively, for VG68 oil lubrication. These

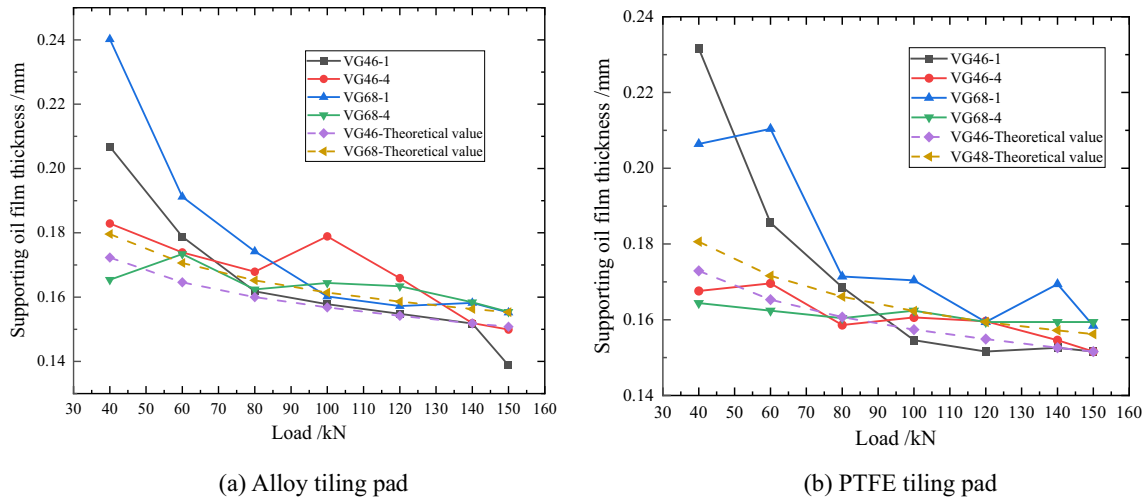


Fig. 10 Comparison of film thickness at bearing pivot point for different tiling pad surface materials

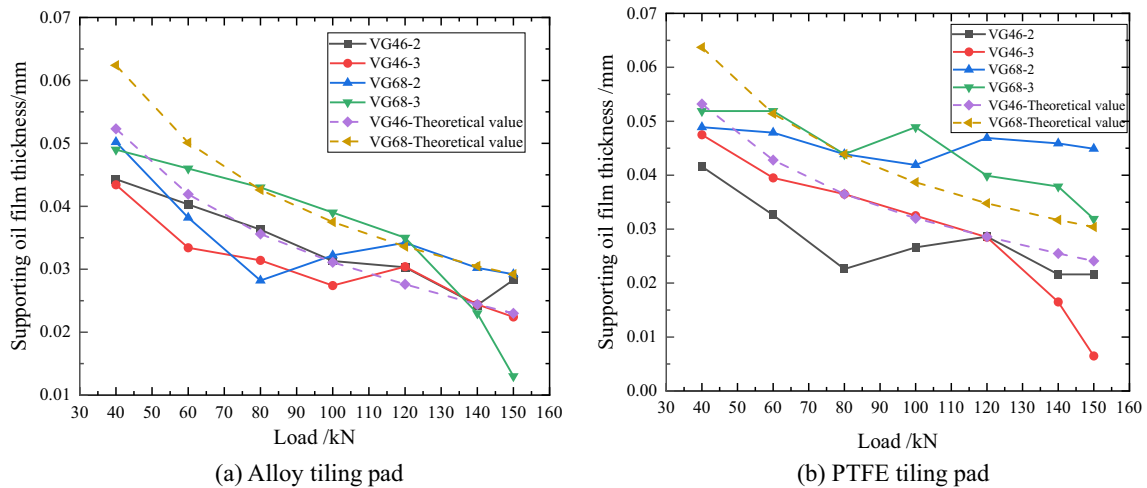


Fig. 11 Comparison of film thickness at bearing pivot point for different tiling pad surface materials

values are close to theoretical calculations, showing consistent variation patterns.

### 4.2 Tiling pad temperature test results and analysis

The comparative data of the bearing pad measurement point temperatures between the test results and theoretical values for bearings with different pad materials (points 1 and 4) are shown in Fig. 12. As the load increases, the measured values of the bearing pad temperatures increase. The temperature values for VG68 oil are generally higher than those for VG46 oil, and the temperature for plastic pads is lower than that for alloy pads. In the load range of 40–150 kN, the temperature at the measurement points on alloy pads lubricated with VG46 oil increased from about

32 °C to about 33.5 °C, with small fluctuations in the 80–100 kN range. For VG68 oil, the temperature increased from 32.5 to 34 °C. Both oil types showed variation patterns close to theoretical calculations, with a difference of about 2 °C. For plastic pads, the temperature at the measurement points with VG68 oil increased from 33.2 to 35.2 °C. Probe 1 and probe 4 had average measurement errors compared to the theoretical averages of 7.2% and 8.0%, respectively, for VG46 oil lubrication and 7.7% and 7.4%, respectively, for VG68 oil lubrication. With VG46 oil, the overall trend increased steadily with load, with a sudden change observed at 80–100 kN for pad 4, followed by a smoother trend beyond 100 kN. The test values were close to theoretical calculations, showing consistent variation patterns.

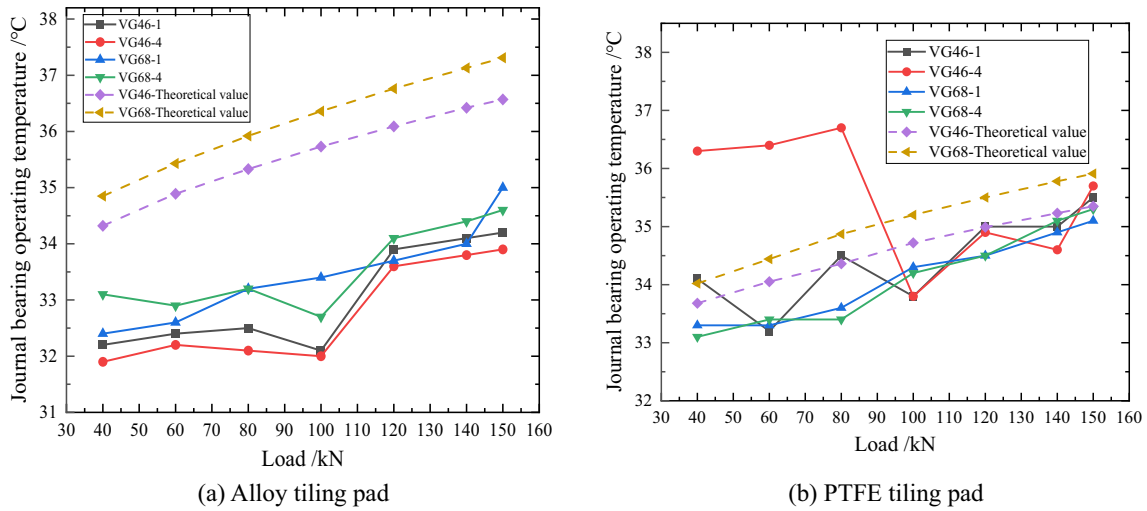


Fig. 12 Comparison of operating temperature of tiling pad with different surface materials (1 and 4)

The change patterns for both oil types are close to the theoretical calculation values. The VG46 oil's temperature is consistent with the theoretical value, while the VG68 oil's temperature differs by about 2 °C, showing slight variations in the 40–50kN range.

The comparative data of the bearing pad measurement point temperatures between the test results and theoretical values for bearings with different pad materials (points 2 and 3) are shown in Fig. 13. As the load increases, alloy tiling pad measured point temperature value tends to stabilize; PTFE tiling pad measured point temperature gradually increased; PTFE tiling pad measured point temperature than the alloy tiling pad as a whole was lower than the 0.5°C; load 40–150kN range: The temperature at the VG46 oil alloy tiling pad measurement point increases from approximately

32.1 to 33.2°C, while the VG68 oil alloy tiling pad measurement point temperature increases from 33.6 to about 34.2°C, which is about 1°C higher than that of VG46. The test results of the two kinds of oils are about 4.27°C lower than the theoretical value. Probe 2 and probe 3 had average measurement errors compared to the theoretical averages of 8.5% and 8.2%, respectively, for VG46 oil lubrication and 8.7% and 8.8%, respectively, for VG68 oil lubrication. For the load range of 40–150 kN on PTFE blocks, the temperature at the measurement points of the blocks increased from 33.5 to 35°C with VG46 oil lubrication and from 33.9 to 36.4°C with VG68 oil lubrication. The deviations in the film thickness at the pivot points for probe 1 and probe 4 from the theoretical values were 2.0% and 2.2%, respectively, with VG46 oil lubrication and 2.8% and 2.5%, respectively, with VG68

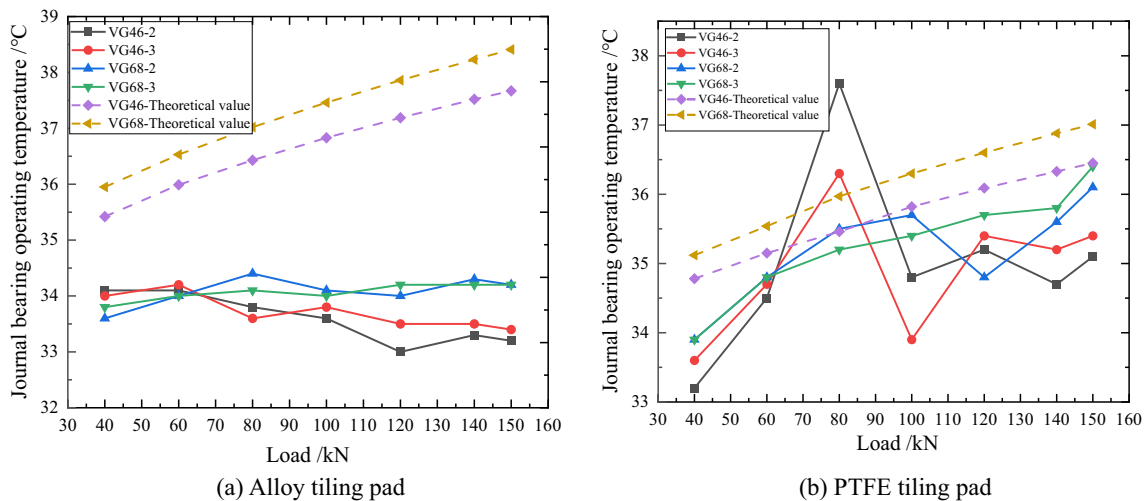


Fig. 13 Comparison of operating temperature with different surface materials (2 and 3)

oil lubrication. These deviations are close to the theoretical calculations and follow the same trend. There was a sudden change in the temperature at the measurement points of the blocks with VG46 oil lubrication between 80–100 kN. The experimental values are close to the theoretical calculation results, and considering the assumptions related to installation and bearing boundary constraints, the error values are within the acceptable range.

### 4.3 Vibration test results and analysis

Under different lubricating oil conditions, the vibration test results of the Babbitt alloy pad bearings and PTFE tiling pad bearings are shown in Figs. 14 and 15. Under the same lubricating oil, the amplitude of horizontal and vertical vibration

tends to be stable with the change of load, and the change of load has little influence on the amplitude of horizontal vibration of the rotor of the different bearings, and the value of vibration of the VG68 oil is about 3 mm/s, which is much larger than that of the VG46 oil, which is 1 mm/s. In the initial stage of applying load (40–150kN), vertical vibration experiences significant fluctuations, first increasing and then decreasing near 100 kN, where it tends to stabilize. Due to the large, short rotor of this test rig (journal diameter D500 mm; length-to-diameter ratio less than 8), the rotor system exhibits rigid rotor behavior (operating speed below the critical speed). The rotor system's vibration is sensitive to external structural parameters, such as bearing clearance.

Based on the test data, it was found that the pivot oil film thickness, tiling pad temperature measurement point,

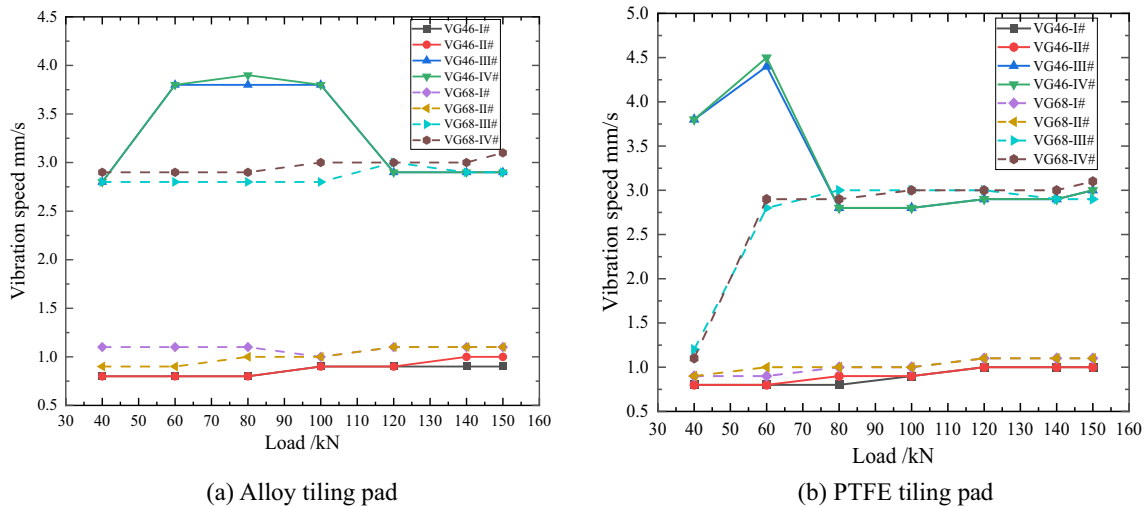


Fig. 14 Comparison of horizontal and vertical vibration of alloy and PTFE with different lubricants (40 rpm)

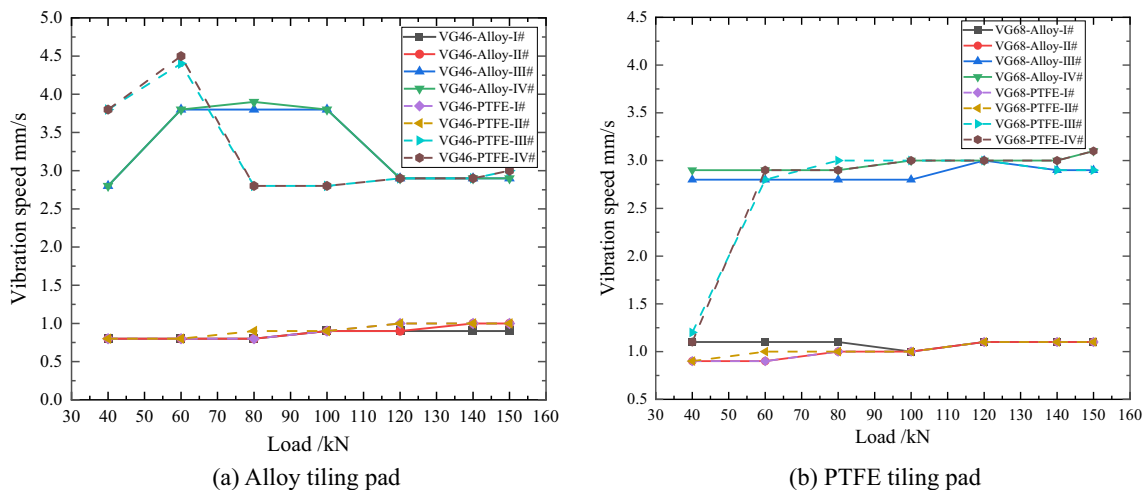


Fig. 15 Comparison of horizontal and vertical vibration of alloy and PTFE with different lubricants (100 rpm)

and vibration values exhibited abrupt changes in the load range of 80–100 kN. Fig. 15 shows the vibration speed at 100 rpm, and it can be seen that the same situation occurs even at high speeds. By considering Fig. 4, which shows the hydraulic loading method and the loading bearing position, this phenomenon can be explained as follows: The center heights of the two loading bearings are unequal, with the left loading bearing being lower and the right loading bearing being higher. As the load increases, the difference in the original center heights is gradually adjusted by the load. Around 100 kN, the rotor tends to level out. Therefore, during the process from 40–100 kN, the center height error decreases from an initial constant value, finally experiencing an abrupt change around 100 kN, with the center height error reducing to zero. This results in the pivot oil film thickness first decreasing and then increasing before 100 kN, while the tiling pad temperature measurement point and bearing box vibration values first increase and then abruptly decrease. This pattern is consistent with the test observations.

## 5 Conclusions

The lubrication performance of bearings, including film thickness and temperature rise, is calculated for an unevenly distributed tilting pad bearing of a large generating unit in service, and a full-scale test rig is established. The pivot film thickness, tiling pad temperature, and vibration data are obtained through tests. The main conclusions are as follows:

- 1) The large tilting pad bearing designed cannot be damaged under low-speed conditions (40 r/min). As the load increases, the thickness of the oil film at the pivot point decreases, the temperature of the tiling pad measurement point increases, and the vibration value is basically unchanged.
- 2) As the load increases, the measured pivot film thickness values of the tilting pads decrease. The average pivot film thickness when lubricated with VG68 oil is greater than that with VG46 oil. The pivot film thickness of the PTFE tilting pads is greater than that of the alloy pads. These measured values are similar to theoretical calculations, and the patterns are consistent.
- 3) As the load increases, the temperature values at the measurement points of the tilting pads increase. The average temperature at the measurement points of the PTFE tilting pads lubricated with VG68 oil is higher than that lubricated with VG46 oil. The temperature at the measurement points of the PTFE tilting pads is lower than that of the alloy pads. These experimental results are similar to theoretical calculations, and the variation patterns are consistent.
- 4) In the same lubricating oil, the amplitudes of the horizontal and vertical vibrations of the bearing housing tend to stabilize with changes in load. The vibration values when lubricated with VG68 oil are greater than those with VG46 oil, and the vertical vibration values are greater than the horizontal vibration values.
- 5) Combined with the experimental arrangement and loading mode, a reasonable explanation is given for the fluctuations in the film thickness of the pivot point, the temperature of the tiling pad measurement point, and the vibration.

**Acknowledgments** This work is supported by Key Research and Development Program of Shaanxi (No. 2024GX-YBXM-209 and No. 2024GX-YBXM-208).

## References

1. Chen B, Wang DH, Liu KP et al (2022) Semi-analytical prediction of the periodic vibration in a sliding bearing-rotor system. *Int J of Non-Linear Mech* 145:104102
2. Chen RL, Tang J, Xu F et al (2023) Influence of oil film nonlinearity on identification accuracy of dynamic characteristic coefficient of heavy-duty sliding bearing. *J Braz Soc Mech Sci Eng* 45(4):233
3. Chatterton S, Pennacchi P, Vania A et al (2019) Cooled Pads for Tilting-Pad Journal Bearings. *Lubricants* 7(10):92
4. Ding AS, Ren XD, Li XS et al (2020) Numerical investigation for characteristics and oil-air distributions of oil film in a tilting-pad journal bearing. *Proc Inst Mech Eng Part J-J Eng Tribol* 234(2):193–204
5. Wagner LF, Allaire PE (2022) Tilting-pad journal bearings-frequency-dependent dynamic coefficients and pivot flexibility effects. *Lubricants* 10(2):20
6. Yan KH, Huang D (2022) Investigation on static and dynamic characteristics of high-speed and heavy-load tilting pad journal bearings[J]. *Industrial Lubr Tribol* 74(9):1063–1073
7. Jin YZ, Yuan XY (2020) Analytical method for hydrodynamic force in finite-length tilting-pad journal bearing including turbulence effect. *J Tribol-Trans Asme* 142(9):091802
8. Lara-Molina FA, Cavalini AA, Steffen V et al (2019) Tilting-pad journal bearing subjected to fuzzy type-2 uncertain parameters. *J Vib Acoust-Trans Asme* 141(6):061008
9. Urbiola-Soto L (2021) Influence of manufacturing variation on the dynamic and tribological performance of tilting pad journal bearings. *J Eng Gas Turbines Power-Trans ASME* 143(6):061017
10. Girish H, Pai R (2021) Effect of journal misalignment on the static characteristics of an innovative journal bearing with adjustable elements in load-on-pad and load-between-pad configurations. *Eng Comput* 38(4):1513–1531
11. Jamali HU, Sultan HS, Abdullah OI et al (2023) Analysis of modified finite length journal bearing under position perturbation. *Lubricants* 11(4):173
12. Ren TM, Feng M (2023) Theoretical and experimental study on the stability of water lubricated high speed journal bearing with lobe pockets. *Tribol Int* 187:108665
13. Stottrop M, Buchhorn N, Bender B (2022) Experimental investigation of a large tilting-pad journal bearing-comparison of a flooded and non-flooded design. *Lubricants* 10(5):83

14. Zywica G, Olszewski A, Baginski P et al (2023) Theoretical analysis and experimental tests of tilting pad journal bearings with shoes made of polymer material and low-boiling liquid lubrication. *Tribol Int* 189:108991
15. Koosha R, San AL (2019) Effect of pad and liner material properties on the static load performance of a tilting pad thrust bearing. *J Eng for Gas Turbines Power-Trans Asme* 141(12):121007
16. Xu JM, Jia Q, Zhang F et al (2018) Fundamental tribological experiments and antifriction design of novel superconducting tilting pad bearing for liquid rocket engine. *Proc Institution Mech Eng Part J-J Eng Tribol* 232(5):582–591
17. Podrabinnik P, Gershman I, Mironov A et al (2023) Study of adaptation processes in tribofilms during friction of antifriction aluminum alloys for journal bearings. *Metals* 13(12):1936
18. Madej M, Leszczynska-Madej B (2023) Analysis of the effect of the chemical composition of bearing alloys on their wear under wet friction conditions. *Lubricants* 11(10):426
19. Mosleh AO, Kotova EG, Kotov AD et al (2022) Bearing aluminum-based alloys: microstructure, mechanical characterizations, and experiment-based modeling approach. *Materials* 15(23):8394
20. Guglielmo G, Enrico M, Andrea R (2022) Efficient flexible multibody models for tilting pad journal bearings. *Machines* 10(4):223–223
21. Yujun W, Georg J, Florian K et al (2023) Investigation of micro-flow effects in textures on hydrodynamic performance of journal bearings using cfd simulations. *Lubricants* 11(1):20–20
22. Hu Y, Masuda T, Yoshimine C et al (2021) theoretical and experimental investigations on directly lubricated tilting pad journal bearing under starved lubrication. *Tribol Trans* 64(4):616–632
23. Ganesha A, Pai RG, Rao S et al (2021) Multi-objective optimization and significant analysis of bearing element adjustments on the static performance of an innovative adjustable bearing through design of experiment. *Proc Institution Mech Eng Part J-J Eng Tribol* 235(9):1820–1833
24. Zhang C, Yi Z, Zhang Z (2000) THD Analysis of high speed heavily loaded journal bearings including thermal deformation, mass conserving cavitation, and turbulent effects. *ASME J Tribol* 122:597–602
25. Faulkner LL (2005) *Rotordynamics*. CRC Press, London

**Publisher's Note** Springer Nature remains neutral with regard to jurisdictional claims in published maps and institutional affiliations.

Springer Nature or its licensor (e.g. a society or other partner) holds exclusive rights to this article under a publishing agreement with the author(s) or other rightsholder(s); author self-archiving of the accepted manuscript version of this article is solely governed by the terms of such publishing agreement and applicable law.